JURNAL INFOTEL
VOL. 16, NO. 4, NOVEMBER 2024, PP. 778–792. DOI:10.20895/INFOTEL.V16I3.1261

RESEARCH ARTICLE

Design and Implementation of Current Control for Step Up-Down Zeta H-Bridge Inverter Using STM32F407VET6

Jonathan Wijaya[1,*], and Leonardus Heru Pratomo[2]

[1,2]Department of Electrical Engineering, Seogijapranata Catholic University, Semarang City 50234, Indonesia

*Corresponding email: wijayajonathan84@gmail.com

Received: October 18, 2024; Revised: November 19, 2024; Accepted: November 25, 2024.

Abstract: The development of electrical power conversion equipment is increasing, along with the utilization of new and renewable energy sources. Power conversion equipment from DC to AC voltage, known as inverters, is extensively researched and implemented in this sector. These inverters commonly operate as step-down voltage in specific applications used as step-ups with limited operating ranges. A step-up-down inverter with a single power circuit is developed to overcome this issue. Still, the number of power switches used correlates with the complexity of its control strategy. This paper investigates a step-up-down inverter using the Zeta H-Bridge Inverter with the implementation of six power switches. Furthermore, this type of inverter is operated with a controlled output current utilizing the STM32VET407 micro controller. The control method is derived based on possible operational modes. An HX10-P current sensor detects the output current. It maintains itself according to the current reference by installing a proportional-integral controller. The initial verification utilizes computational simulation with power simulator software, ensuring the system operates as intended. The final stage involves implementation in the laboratory and testing with standardized equipment. The test results meet the IEEE 519 standard, where the output current has a THD of 1.1%.

Keywords: Current Balancer, Current Control, H-Bridge Inverter, Step Up-Down, ZETA Converter

© Jurnal Infotel ISSN: 2085-3688; e-ISSN: 2460-0997

1 Introduction

The development of electrical power engineering is proliferating, especially in renewable energy, due to environmental issues in offices, housing, and the industrial sector [1]. The increasing energy demand is particularly felt with the rise in fuel prices. Therefore, more research is focusing on alternative energy, also known as environmentally friendly energy. There is already much-related research using alternative energy as a source of electricity generation [2]. Environmentally friendly alternative energy is obtained from various sources, such as wind, water, and solar [3]. These energies produce DC output voltage, but the voltage commonly used is in the form of AC, so equipment is needed to convert the energy with high efficiency, simplicity, and low cost.

Previous research on the step-up-down voltage converter is known as the Zeta Converter [4]. Modification of Zeta Converter topology by using two inductors and two capacitors to achieve better performance has been studied and implemented [5–7]. The Zeta Converter is a step-up-down voltage converter with several advantages, such as low output voltage ripple and the same polarity as the input voltage [4,8]. Other power converters are CUK and SEPIC converters, where three converters are superior to conventional step-up-down converters [9, 10]. The Zeta Converter is widely used with the Continuous Conduction Mode (CCM) switching method, thus generating Pulse Width Modulation (PWM) with a duty cycle that never reaches zero [4, 11]. As in the research developed by several researchers [12], a Zeta converter is utilized for current control. Another utilization of the Zeta Converter is used to maximize the output and efficiency of Maximum Power Point Tracking (MPPT) in Photovoltaic applications. The H-Bridge inverter is a DC-AC converter controlled by a single leg that has been tested and works well using the Voltage Source Inverter (VSI) method [13]. With sinusoidal pulse width modulation (SPWM) switching mode, the H-Bridge Inverter topology produces a suitable output voltage [14, 15]. Controlled current H-Bridge Inverter can produce better power quality with Total Harmonic Distortion (THD), according to IEEE Std 519-2014 [16–18]. This topology uses current control strategies to control the output current even under load variations [19, 20]. AC-AC Converter is one of the topologies for changing the output voltage amplitude developed by several researchers [17, 21]. This paper aims to combine two inverter topologies and Zeta converters to form a new type of inverter. Combining the H-Bridge inverter and Zeta converter enables it to operate over a wide range. This topology uses six power switches consisting of 4 power switches for the H-Bridge Inverter and two for Zeta AC-AC.

The proposed topology of an H-Bridge-based inverter and Zeta AC-AC converter is based on operation modes to obtain a new control structure. Furthermore, this new topology of the H-Bridge inverter and Zeta AC-AC converter is operated as a controlled current source inverter. The new inverter topology, operation modes, and control strategies are further discussed in section 2. Simulation results, hardware testing in the laboratory, and detailed analysis are discussed in section 3. Conclusions based on the simulation results and implementation are presented in section 4.

2 Research Method

The proposed topology uses the H-Bridge Inverter and Zeta Converter. Zeta AC-AC operates on AC voltage as a step-down and step-up output voltage. Figure 1 shows the Zeta H-Bridge Inverter topology with six active power switches.

2.1 Zeta H-Bridge Inverter

This section explains the operation of the Zeta H-Bridge Inverter using the switching strategy during the positive cycle. When switches S1 and S4 conduct and S2 and S3 are inactive, the H-Bridge Inverter produces an output voltage $V_{L1} = V_s$. During the negative cycle, S2 and S3 conduct while S1 and S4 are inactive, resulting in an output voltage of $V_{L1} = -V_s$. Figure 1 shows the proposed Zeta H-Bridge Inverter Topology by combining the H-Bridge Inverter with the Zeta Converter. Figure 2 illustrates the operational mode using four power inverter switches (S1 - S4) and two Zeta AC-AC power switches (S5 and S6).

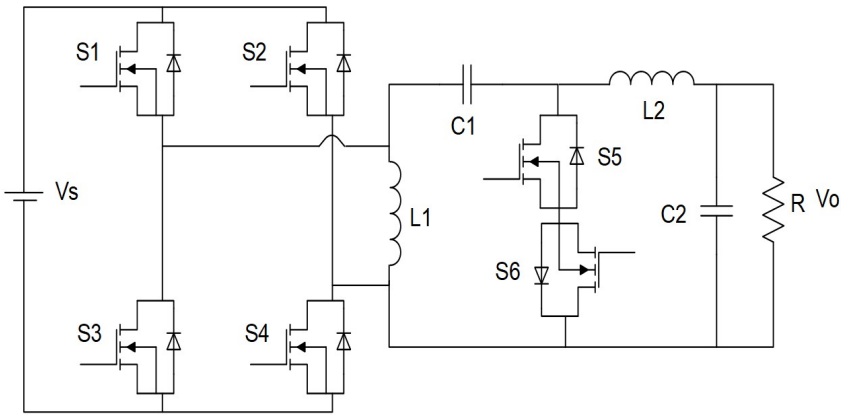

Figure 1: Zeta H-Bridge inverter.

Two operating modes are shown in Figure 2 for a positive cycle, where:

1. The operation of the inverter power switch occurs during the positive cycle, with S1 and S4 conducting. At this point, when the voltage is up to (V_s), the current flows from the DC source (V_s) towards L1 and then back to (V_s). According to KVL (Kirchoff's Voltage Law), the current in the inductor can be derived from the equation:

$$V_{L_1} = V_s = L_1 \frac{dil_1}{dt} \tag{1}$$

$$\frac{dil}{dt} = V_s / L_1 \tag{2}$$

The instantaneous change in the current value of inductor L1 while switches S1 and S4 are conducting is:

$$\Delta I_{L1_{on}} = \int_0^{DT} dIL_1 = \frac{V_s DT}{L} \tag{3}$$

2. When the Zeta AC-AC power switch is working, and S6 is conducting, the current in inductor L1 will flow towards the load and then return to L1 and L2 with S6 active and S5 operating as a diode. This condition is called freewheeling, and the following equation applies:

$$V_{L_1} = V_o = L\frac{dil_1}{dt} \tag{4}$$

$$\frac{dil_1}{dt} = \frac{V_o}{L_1} \tag{5}$$

So, the value of the instantaneous current change in inductor L1 during the activation of switch S6 or freewheeling mode is as follows:

$$\Delta I_{L1_{off}} = \int_0^{(1-D)T} dIL_1 = \frac{V_o(1-D)T}{L} \tag{6}$$

The total energy stored in an inductor during both conduction and non-conduction in one cycle is equal to zero (0):

$$\Delta_{L1_{off}} + \Delta_{L1_{on}} = 0 \tag{7}$$

Equation 8 and Equation 9 are obtain by substituting the above Equation 3 and Equation 6:

$$\Delta_{L1_{off}} + \Delta_{L1_{on}} = \frac{V_o(1-D)T}{L} + \frac{V_s DT}{L} = 0 \tag{8}$$

$$\frac{V_o}{V_s} = \frac{D}{1-D} \tag{9}$$

where D is modulation Index.

2.2 Switching Control Strategy

The SPWM control strategy generates the switching signals for the power switches in the inverter section. This SPWM control is derived from the control strategy illustrated in Figure 3. Figure 3 illustrates the SPWM control strategy using two sinusoidal signals (Vsin) that are phase-shifted oppositely (-Vsin) and modulated with a triangular carrier signal. This modulation produces an SPWM switching pattern where S1 and S4 switch during the positive cycle, while S2 and S3 switch during the negative cycle. S5 and S6 are zero-crossing PWM signals complementary and operate at a 50 Hz frequency. It is obtained by comparing Vsin with zero.

2.3 Current Control Strategy

The experiment conducted to test this topology employs an output current control strategy. Several control methods, such as Hysteresis, Proportional, and others, can be used. In this test, a Proportional Integral (PI) controller is used due to several advantages, including the predictability of the switching frequency, as it uses a triangular carrier signal. Moreover, this type of control has a fast response time, allowing it to achieve the desired output signal by the reference signal, even with load variations. The PI control structure is shown in Figure 4.

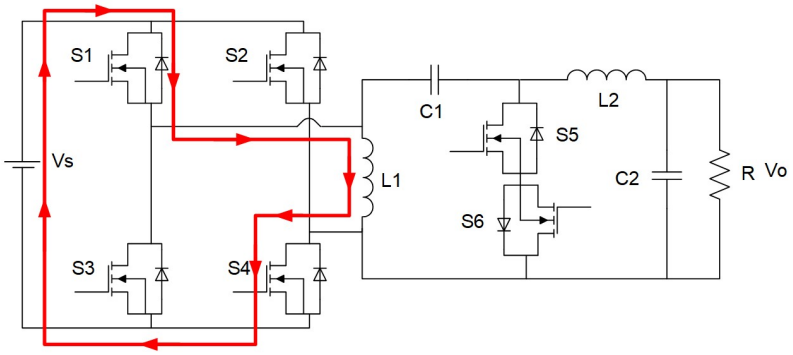

(a) mode 1

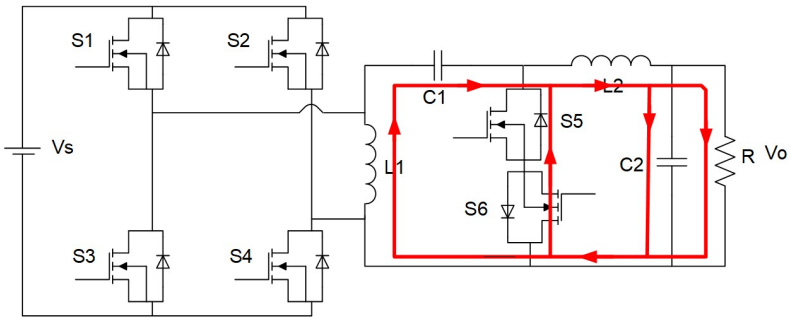

(b) mode 2

Figure 2: Two operation modes of the Zeta H-Bridge inverter.

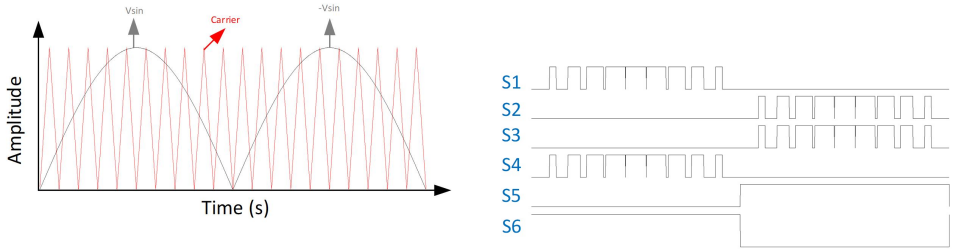

(a) SPWM modulation (b) Signal SPWM and PWM

Figure 3: Control strategy SPWM.

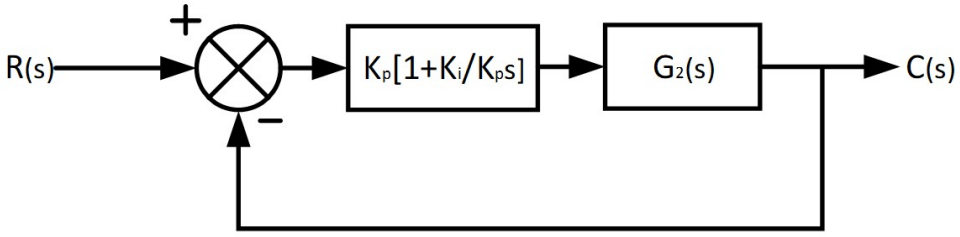

Figure 4: Proportional Integral (PI) control strategy.

K_p is the proportional gain, K_i is the integral gain, and $C(s)$ represents the output of the controlled system, also known as $Iact$. The values of K_p and K_i are adjusted during field implementation to achieve the desired error value. The error is defined as the difference between the reference value R(s) and the actual value $C(s)$, and it is formulated as shown in Equation (10).

$$\text{error} = R(s) - C(s) \tag{10}$$

Figure 5 represents this paper's proposed output current control strategy circuit. The Current Transducer HX-10P is used as the sensor for Iout. The output from the HX-10P provides the actual system value Iout, which is then converted into a voltage scale for the STM32F407VET6 microcontroller to generate the error value. The PI values obtained from computational simulations using power simulator software are compared with a high-frequency triangular signal of 10 kHz. This results in SPWM switching with a 180° phase shift between the positive and negative cycles. The AC-AC Zeta switching uses the PWM Zero Crossing method with inverted switching, ensuring that the positive and negative cycle switches do not turn on simultaneously. Figure 6 shows the programming algorithm used for the control strategy illustrated in Figure 5. The IR2111 optocoupler is used to simplify programming, as only one program needs to be written for the same inverter leg, with the lower switch being the complement of the upper switch.

2.4 Components and Parameter

The Zeta H-Bridge Inverter circuit utilizes six MOSFETs as power switches (IRF450). The STM32F407VET6 microcontroller generated the switching signals algorithm based on Figure 6. The switching signals from the microcontroller are sent to four TLP250 optocouplers and two IR2111 optocouplers, which act as signal transmitters to the power switches. The output current was detected by the current sensor (HX10-P), and it was used for feedback current. The Audio Frequency Generator (AFG) was used for reference signals that would be controlled. Table 1 lists the components and parameters used in both simulation and hardware implementation. Figure 7 shows the electrical circuit block diagram that was designed based on Figure 5 and Figure 6. The electrical circuit block diagram implemented by electronic devices is described above. Figure 8 shows the hardware implementation of the Zeta H-Bridge Inverter in laboratory tests based on Figure 7.

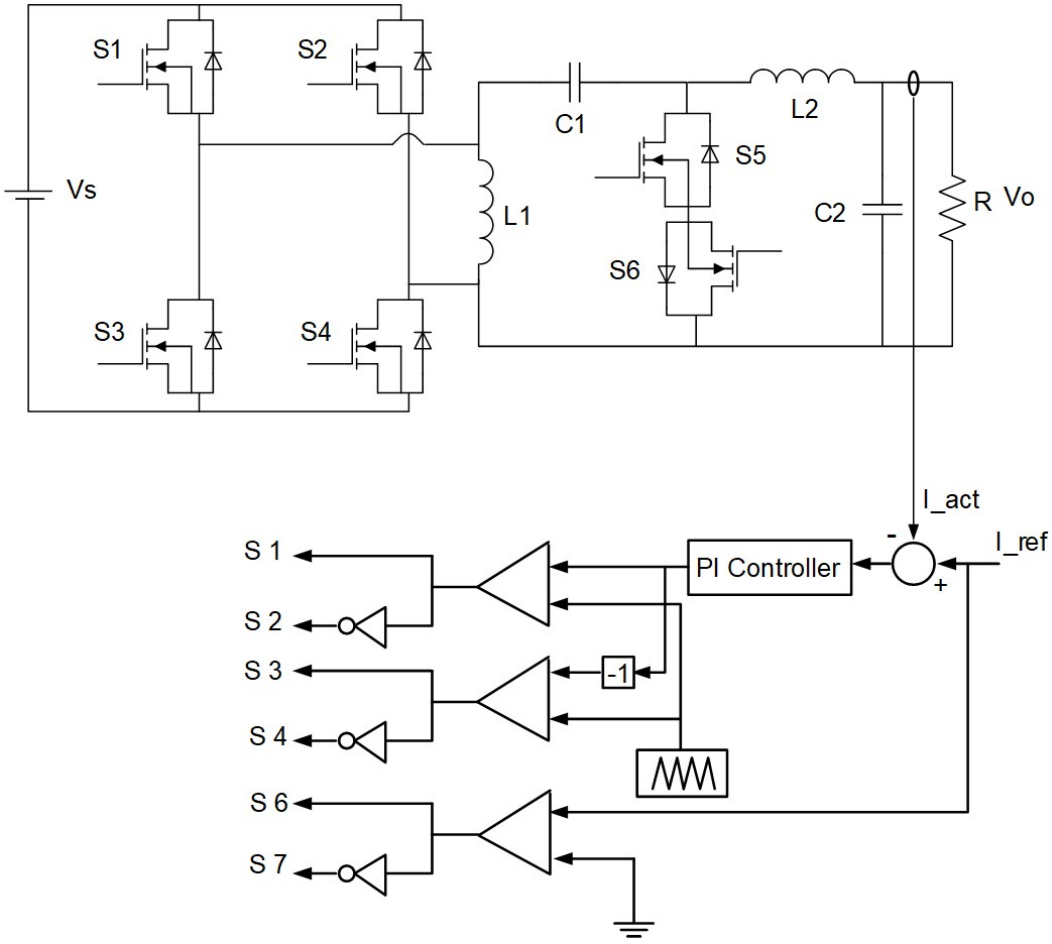

Figure 5: Topology of current controlled Zeta H-Bridge inverter strategy.

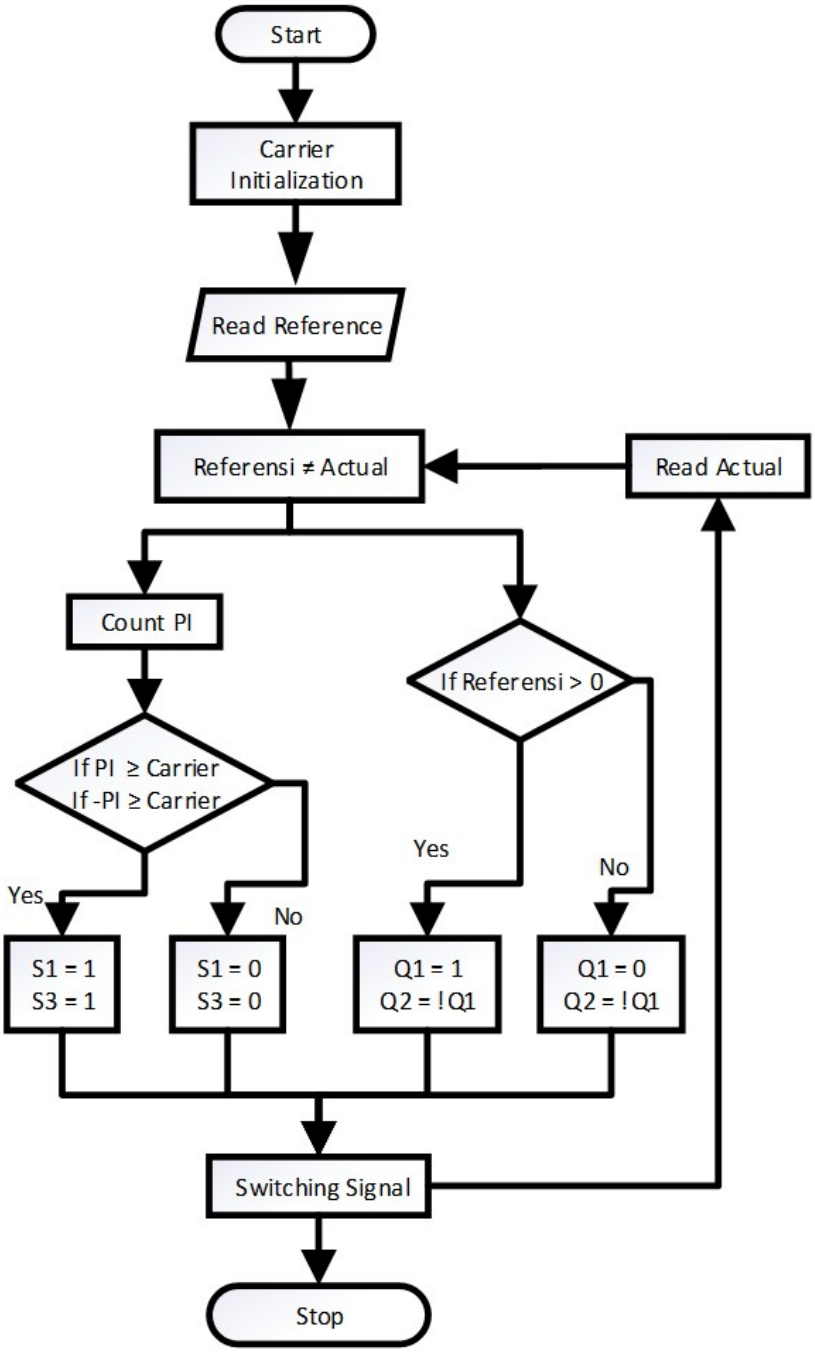

Figure 6: Flowchart of program algorithm.

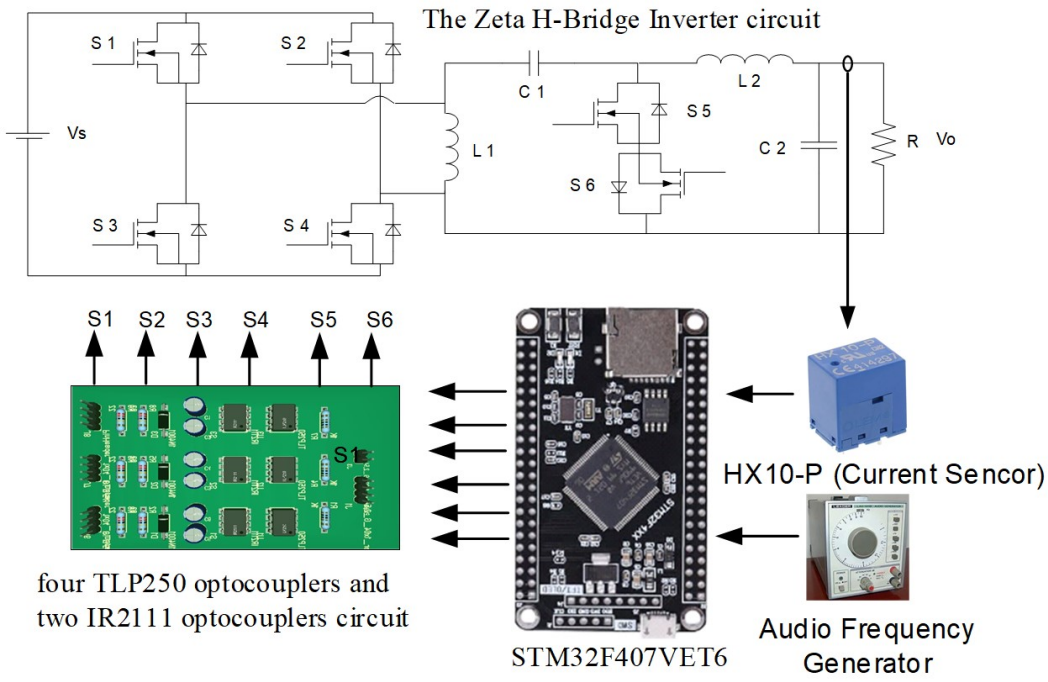

Figure 7: The electrical circuit block diagram.

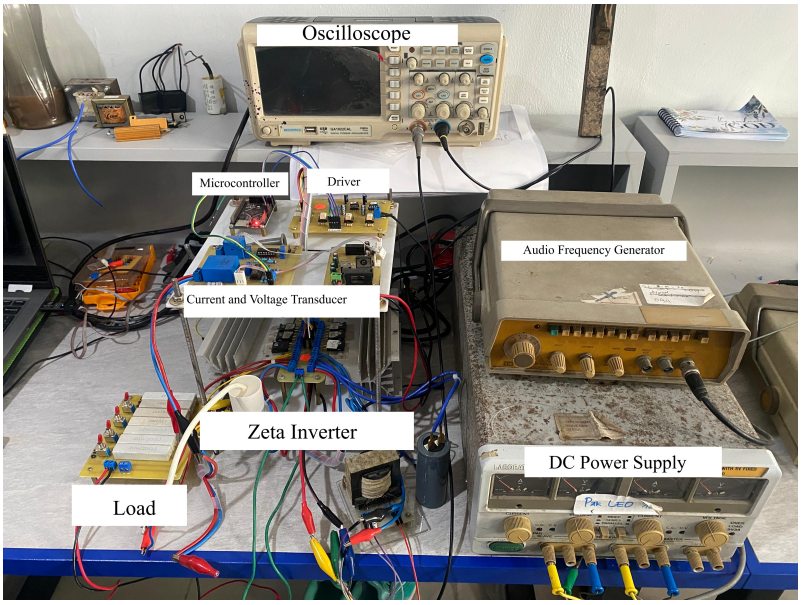

Figure 8: Hardware implementation.

Table 1: Parameters

No	Components	Value
1	DC Source	12V
2	Inductor 1	2mH
3	Inductor 2	0.2mH
4	Capacitor 1	100uF
5	Capacitor 2	10uF
6	Load	50-100Ω
7	Gain Proportional	20
8	Gain Integral	0.001
9	Switching Frequency	10KHz

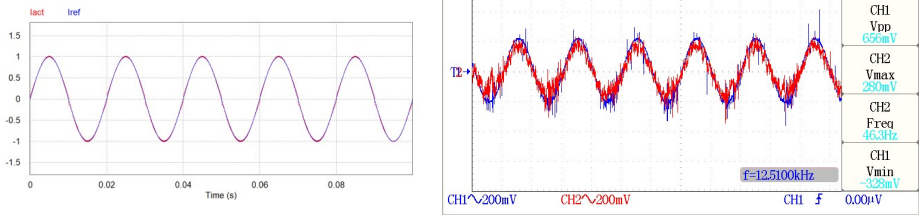

(a) Simulation (b) Implementation

Figure 9: Iact and Iref measuring wave during step-down condition.

3 Results and Discussion

To verify the results of the laboratory testing and simulation, the same parameters and components listed in Table 1 were applied, yielding consistent outcomes. This topology was developed to allow testing under both step-up and step-down voltage conditions by adjusting the value of Iref. The higher Iref value accepted by the STM32F407VET6, the higher the output voltage compared to the input voltage (voltage step-up). Conversely, reducing Iref results in a lower output voltage (voltage step-down). During the simulation of the step-down condition, as shown in Figure 9a, the actual current Iact consistently follows Iref. Iact also follows Iref in the hardware implementation, as shown in Figure 9b. It demonstrates that the hardware implementation and simulation results are aligned and correlated, as can be compared in Figure 9a and Figure 9b.

The simulation results show the output voltage and current under voltage reduction conditions, displayed within a single frame, indicating that the voltage and current phases are the same, as shown in Figure 10a. it is then tested in the implementation depicted in Figure 10b. The voltage step-down condition is evaluated by comparing the output voltage amplitude with the input DC voltage. Figure 11a shows the simulation results tested under the step-down condition. Figure 11b presents the implementation results, indicating that the amplitude of the AC output cannot exceed the input voltage.

Based on the voltage step-up condition, the measurements were close to the step-down condition. In the simulation results shown in Figure 12a, the current actual (Iact) was

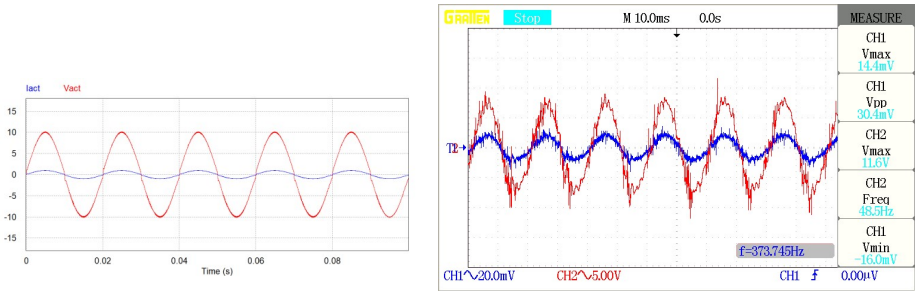

(a) simulation (b) implementation

Figure 10: Vout and Iout measuring wave step-down condition.

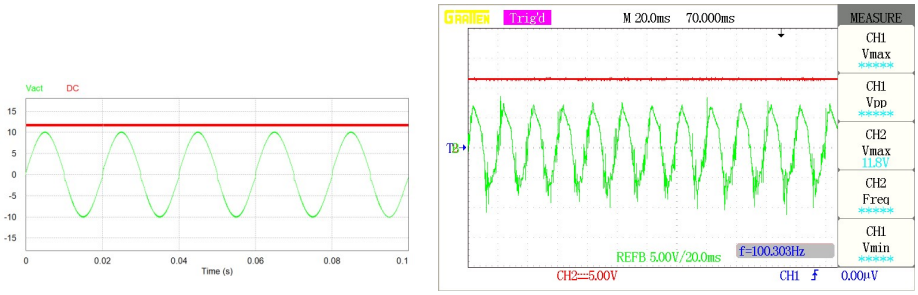

(a) simulation (b) implementation

Figure 11: Vin and Vout measuring wave during step-down condition.

locked to the current reference (Iref). The hardware implementation test is shown in Figure 12b: the current actual (Iact) was followed by the current reference (Iref). Figure 13a shows Vout and Iout during simulation and implementation under the voltage step-up condition, Figure 13b. This comparison verifies that the output voltage and current are in phase.

To test the step-up condition, the amplitude of the AC output voltage or Vout was compared with the DC input voltage or Vin in both simulation and implementation. The amplitude of Vout must be higher than the Vin to prove that topology can work at the step-up condition: simulation Figure 14a and implementation, Figure 14b. For testing the current-controlled topology, the load was varied between 50Ω to 100Ω, Table 1. When the load changes, the Iout remains stable while the Vout changes the amplitude. This is because the control strategy used is current control, which is designed to stabilize the current under all conditions, such as load changes. Figure 15a shows the simulation result tested under the load changes. Iout will not change under the load changes, while Vout will change as the load changes. Figure 15b shows the hardware implementation result. Figure 16 shows a Total Harmonic Distortion (THD) value of 1.1% for both the output voltage and current. This value meets the IEEE Std 519-2014 standard, which requires THD to be less than 5%. Low THD is crucial for power converter topologies to ensure that current is injected into the grid with minimal distortion.

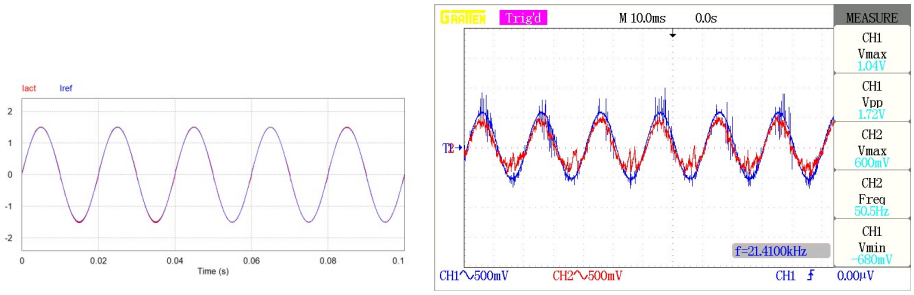

(a) simulation (b) implementation

Figure 12: Iact dan Iref measuring wave during step-up condition.

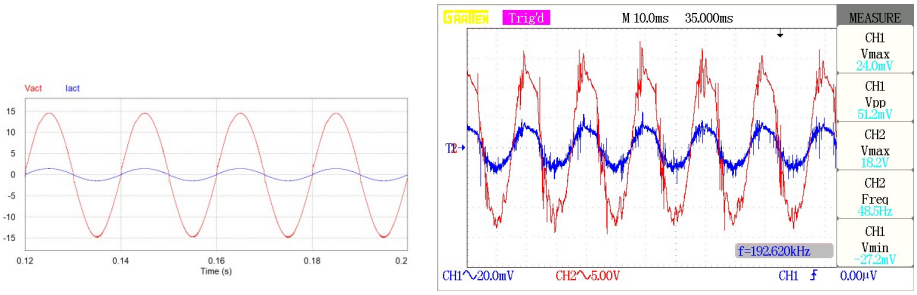

(a) simulation (b) implementation

Figure 13: Vout dan Iout measuring wave during step-up condition.

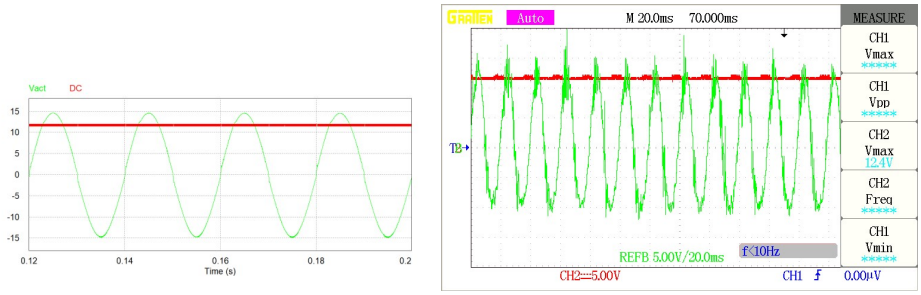

(a) simulation (b) implementation

Figure 14: Vin dan Vout measuring wave during step-up condition.

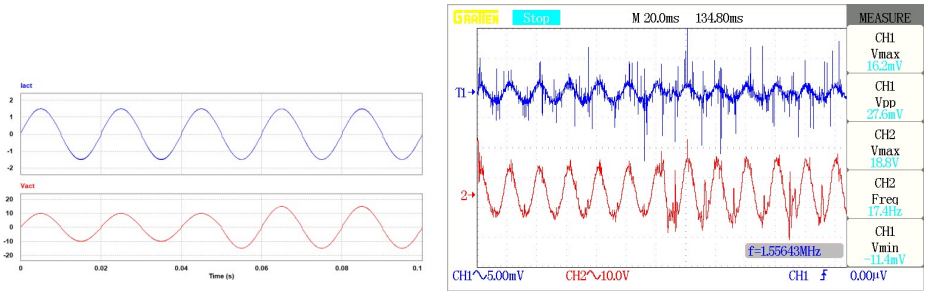

(a) simulation (b) implementation

Figure 15: Iout dan Vout when load changes.

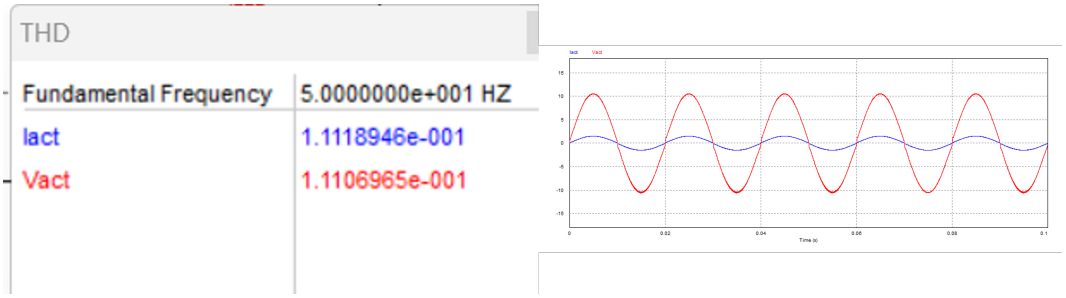

Figure 16: Total harmonic distortion value at current and voltage output.

4 Conclusion

The current-controlled Zeta H-Bridge Inverter topology combines an H-Bridge Inverter with an AC-AC Zeta converter, where the output current is controlled, allowing it to operate effectively as both a voltage step-up and step-down converter using six power switches. The topology can switch between step-up and step-down conditions by adjusting the amplitude of Iref, enabling dual-mode operation. Load variation tests demonstrated that the current control can stabilize the output current under changing load conditions. As a result, this topology achieves high efficiency and low THD, with measured THD values of 1.11% for the output current and 1.11% for the output voltage.

References

[1] L. Pratomo, S. Paudel, and B. Cahyadi, "A simple method for controlling buck-boost sepic h-bridge inverter," *International Journal of Applied Power Engineering (IJAPE)*, vol. 13, p. 670, 09 2024.

[2] S. Paul, T. Dey, P. Saha, S. Dey, and R. Sen, "Review on the development scenario of renewable energy in different country," in *2021 Innovations in Energy Management and Renewable Resources (52042)*, pp. 1–2, IEEE, 2021.

[3] I. J. Hashim, "A new renewable energy index," in *2021 6th International Conference on Renewable Energy: Generation and Applications (ICREGA)*, pp. 229–232, IEEE, 2021.

[4] F. L. de Sa, C. Dal Agnol, W. Raphael, D. R. Caballero, and S. A. Mussa, "A new dc-dc double zeta quadratic converter," in *2020 IEEE International Conference on Industrial Technology (ICIT)*, pp. 426–431, IEEE, 2020.

[5] M. Ghavaminejad, E. Afjei, and M. Meghdadi, "Double-input/single-output zeta converter," in *2021 12th Power Electronics, Drive Systems, and Technologies Conference (PEDSTC)*, pp. 1–5, 02 2021.

[6] B. Hosur, "Design and simulation of zeta converter for speed control of bldc motor," *International Journal of Emerging Technologies in Engineering Research (IJETER) Volume*, vol. 7, 2019.

[7] F. D. Murdianto, I. Sudiharto, and E. Wulandari, "Performance evaluation zeta converter using pi controller for energy management in dc nanogrid isolated system," *INTEK: Jurnal Penelitian*, vol. 8, no. 1, pp. 37–42, 2021.

[8] H. Suryoatmojo, A. Rifa'i, D. Riawan, E. Setijadi, S. Anam, R. Mardiyanto, and M. Ashari, "Application of high gain zeta converter for photovoltaic system," in *2019 International Seminar on Intelligent Technology and Its Applications (ISITIA)*, pp. 144–149, IEEE, 2019.

[9] S. Sharma and R. Diwan, "Zeta converter with pi controller," *Int. J. Eng. Trends Technol*, vol. 67, no. 2, pp. 33–36, 2019.

[10] J. A. Ziani, M. J. B. Ghorbal, and S. Moussa, "Comparative study of boost and zeta converters in dc microgrid applications," in *2020 6th IEEE International Energy Conference (ENERGYCon)*, pp. 222–225, IEEE, 2020.

[11] M. Ghavaminejad, E. Afjei, and M. Meghdadi, "A study on applying interleaved switching pattern on a double-input/single-output zeta converter," in *2021 12th Power Electronics, Drive Systems, and Technologies Conference (PEDSTC)*, pp. 1–5, IEEE, 2021.

[12] M. Arora, "Output current sensor based maximum power point tracking with load protection for pv system using zeta converter," in *2021 International Conference on Control, Automation, Power and Signal Processing (CAPS)*, pp. 1–6, IEEE, 2021.

[13] A. Srivastava and J. Seshadrinath, "Common mode leakage current analysis of 1ϕ grid-tied transformer less h-bridge pv inverter," in *2021 International Conference on Sustainable Energy and Future Electric Transportation (SEFET)*, pp. 1–6, IEEE, 2021.

[14] E. Rodriguez, G. G. Farivar, N. Beniwal, C. D. Townsend, H. D. Tafti, S. Vazquez, and J. Pou, "Closed-loop analytic filtering scheme of capacitor voltage ripple in multilevel cascaded h-bridge converters," *IEEE Transactions on Power Electronics*, vol. 35, no. 8, pp. 8819–8832, 2020.

[15] K. Tan, H. Wang, and C. Wang, "A decoupling control method for hybrid cascaded h-bridge inverter," in *2020 IEEE 9th International Power Electronics and Motion Control Conference (IPEMC2020-ECCE Asia)*, pp. 2469–2471, IEEE, 2020.

[16] P. K. Behera, A. Satpathy, and M. Pattnaik, "Design and implementation of a single-band hysteresis current controlled h-bridge inverter," in *2020 3rd International Conference on Energy, Power and Environment: Towards Clean Energy Technologies*, pp. 1–6, IEEE, 2021.

[17] C. Ren, L. Liu, X. Han, B. Zhang, L. Wang, and P. Wang, "Multi-mode control for three-phase bidirectional ac/dc converter in hybrid microgrid under unbalanced ac voltage conditions," in *2019 IEEE Energy Conversion Congress and Exposition (ECCE)*, pp. 2658–2663, IEEE, 2019.

[18] K. Franck, B. H. Zacher, S. Holzmann, M. Wagner, and C. Schumann, "Low thd current control of nonlinear load characteristics using a single phase dual zeta inverter," in *2024 IEEE Applied Power Electronics Conference and Exposition (APEC)*, pp. 2342–2347, IEEE, 2024.

[19] K. Ge, Z. Fan, L. Fang, and J. Chen, "Inverter control based on virtual impedance under unbalanced load," in *2020 IEEE 29th International Symposium on Industrial Electronics (ISIE)*, pp. 1167–1172, IEEE, 2020.

[20] H. Zhang, H. R. Wickramasinghe, J. Li, and G. Konstantinou, "Modular multilevel converter operation in passive networks under unbalanced loads," in *2019 IEEE PES GTD Grand International Conference and Exposition Asia (GTD Asia)*, pp. 362–367, IEEE, 2019.

[21] F. Xupeng, M. Tongtong, D. Xiaokang, Z. Shixiang, L. Ji, and L. Fengzhao, "Research on three-phase cascaded quasi-impedance-source ac/ac converter," in *2019 Chinese Automation Congress (CAC)*, pp. 1804–1809, IEEE, 2019.